Evaporation time of liquid droplet on superheating horizontal surface

Mousa M. Mohamed and Ahmed E. Hanafy

Mechanical Power Eng. Dept., Faculty of Eng., Minufiya University, Shebin El-Kom, Egypt

The evaporation time of small liquid droplet on superheating surface was studied analytically. The thickness of vapor layer under the droplet as a function of droplet size, surface superheating, radius of contact area between the droplet and surface, and vapor thermal properties was derived analytically. The rate of droplet diameter decrement and evaporation time were formulated and verified with the experimental data in the literature for water and pure hydrocarbon fuels such as heptane, decane and hexadecane. The tested range of droplets size was 0.068 to 3.04 *mm*, and superheating surface temperatures from Leidenfrost temperature up to 550 *oC*. The prediction of droplet evaporation time for water was within percentage deviation of –17 ~ 4 % than experimental data, while for heptane was within percentage deviation of – 45 ~ 9 % and decane was within percentage deviation of –9 ~ 10 %. The deviation between the experimental data and prediction was ± 35 % for tested liquid droplets. The model developed was in good agreement with the experimental data and the comparison in film boiling region for droplet diameter decrement, evaporation time and time-average droplet heat transfer rate was fairly well.

تم الحصول بالطرق التحليلية على معادلة لتبخير قطرة السائل على سطح أفقى ساخن وتم اختبارها بالنتائج العملية، والقطرة على شكل شبه كروى بمساحة اتصال مستوية بينها وبين السطح الساخن وقد اعتبر أن انتقال الحرارة بالتوصيل من السطح الساخن إلى القطرة خلال طبقة من البخار أسفل القطرة بسمك منتظم. تم بالاستنتاج التحليلى الحصول على سمك طبقة البخار تحت القطرة بحل معادلات الحركة والطاقة واتزان القوى المؤثر على القطرة ، بعد ذلك تم حساب معدل تناقص قطر القطرة نتيجة التبخير بمعادلة الحرارة المنتقلة بالتوصيل عبر طبقة البخار والحرارة اللازمة لتبخير القطرة بالكامل، وقد تم اختبار تبخير قطرات من الماء وأنواع من الوقود الهيدروكربونى مثل الهبتان والديسان والهكساديسان بقطر يتراوح من ٠,٠٥ حتى ٣ مم ودرجة حرارة للسطح الساخن حتى ٥٥٠ ْم. وبوجه عام فإن النموذج الرياضى المقترح ومعادلة زمن تبخير القطرة التى تم الحصول عليها فى منطقة الغليان الغشائى أظهرت تطابق بين الحسابات والنتائج العملية بدرجة مقبولة من الثقة.

Keywords: Droplet evaporation time, Leidenfrost temperature, Droplet diameter decrement, Droplet heat transfer rate, Film boiling

1. Introduction

The evaporation of liquid droplets on heated surface have been widely used in many fields related to various types of combustion to improve combustion efficiency, spray cooling systems and in safety considerations for various types of reactors. Droplet evaporation upon a heated surface at temperature above boiling point involves heat transfer in different modes. The heat transfer characteristics have three distinctive regions according to the surface temperature, the regions associated with nucleate, transition and film boiling. Theoretical and experimental studies were conducted to investigate the evaporation rates and overall heat transfer coefficient of water droplets, which were supported by their own

superheated vapor on a flat surface [1-2]. The water droplet in film boiling region is assumed to have flat disk geometry with a uniform vapor gap, forming an insulating layer between the droplet and heated surface [3-5]. Relations between the shape and the dimensionless volume of droplet in film boiling region were correlated. Comparisons between the correlation and experimental data were made, and some discrepancies for droplet vaporization time and heat flux were found between the prediction and the experimental data especially for small droplets. The effect of surface material and ambient pressure on evaporation time of discrete droplet in film boiling region were studied experimentally [6]. Much attention was made to the wettability and thermal diffusivity of surface as to the heat transfer

characteristics. The evaporation time was decreased as the ambient pressure increased, and Leidenfrost temperature increased with increasing ambient pressure. The Leidenfrost temperature varied with ambient pressure for any given material of heating surface and no single correlation with ambient pressure and surface roughness was obtained. The evaporation characteristics of water in fuel emulsion droplets in film boiling on a heated surface were studied experimentally [7-8]. For heptane-water emulsion droplets, heptane was preferentially evaporated from the droplets, where as for water decane emulsions, water prevaporization occurred before decane. Also, the results showed that the droplet evaporation rate decreased, and the total droplet evaporation time increased with increasing water content.

The droplet evaporation rate and critical heat transfer flux of dispersed water droplets impacting a horizontal heated surface were investigated experimentally [9-10]. A generalized correlation was developed for the critical heat flux as a function of Weber and Strouhal numbers of the impacting droplets and the deviation between predicted and experimental data was less than ± 22 %. A numerical model was developed to conduct a study of single droplet evaporation over a wide range of ambient pressures both under normal and micro-gravity conditions [11]. The droplet lifetime as a function of ambient pressure and initial droplet diameter were presented, and the enhancement in the droplet evaporation rate due to natural convection was more dominant with increasing ambient pressure. A molecular dynamics simulation method was developed to study the evaporation of sub-micron droplets in a gaseous surrounding [12]. An experimental set up was built to investigate the influence of ethanol concentration and droplet profile on the evaporation rate [13]. The evaporation rate measurements indicated that the more volatile component evaporated entirely in the first stage, while the less volatile component was dominantly evaporated in the last stage. The behavior of wetting angle was correlated with the volume of the droplet and the ethanol concentration. The evaporation rate of small water and n-heptane droplets

were observed below the saturation temperature and atmospheric pressure [14]. The evaporation rate and contact angle were calculated and used to predict the heat transfer rate on the heated surface. The results showed that the trends in the wetted diameter, height and contact angle for water droplets were fundamentally different than the geometric changes of n-heptane droplets.

The objective of the present study was to develop a closed correlation for evaporation time and heat transfer rate of small liquid droplet upon a horizontal superheating surface. Also, modification of the vapor layer thickness under the droplet as a function of droplet diameter, superheating surface temperature, radius of contact area and vapor thermal properties were considered. Both the validity and limitation of the correlations of evaporation time and time-average droplet heat transfer rate were examined with the experimental data in the literature for various droplet diameters and surface superheating temperature.

2. Model of droplet evaporation

In the present model, the droplet evaporation and heat transfer rate from the heated surface to the droplet was formulated as shown in fig. 1. The actual shape of the droplet during evaporation is an oval shape with nearly flat bottom and with distance away the heating surface equals δ_m and base radius r_b. The actual droplet volume is equal to hypothetical spherical shape of radius R. The heat transferred to the droplet is mainly by conduction from the heating surface to the bottom of the droplet. Thin vapor layer insulates the lower face of the droplet and the direct contact heat transfer between liquid droplet and the heated surface is negligible in this study. The evaporation due to radiation heat transfer from the heated surface to the lower and upper faces of the droplet, and the mass diffusion from the droplet is small compared to the evaporation rate. The problem is assumed to be quasi-steady at mid-time interval $\delta\tau$ and the unsteadiness effects are neglected.
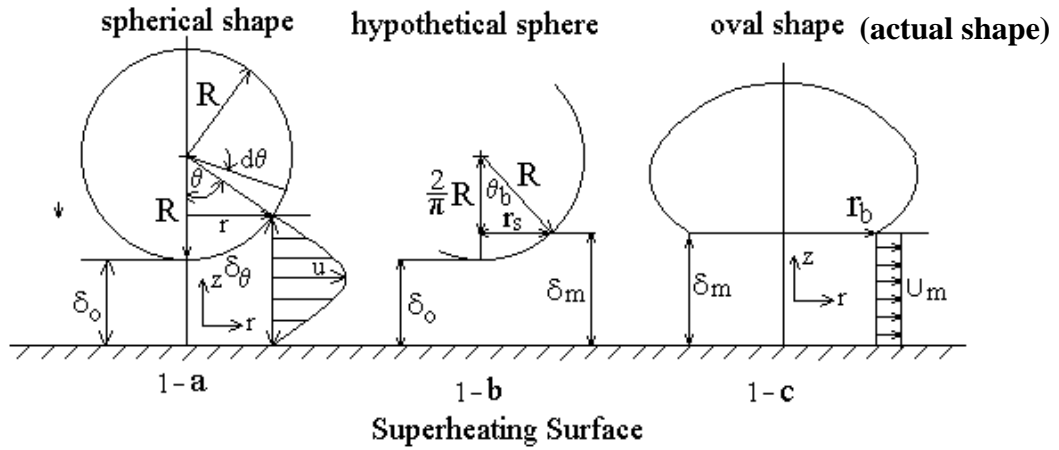
Fig. 1. Model of droplet evaporation in film boiling region.

The geometric relationships of droplet in hypothetical spherical shape fig. 1-a gives relation of mean thickness of vapor layer as follows:

$$\delta_\theta = \delta_o + R - R\cos\theta$$
$$\delta_m = \frac{1}{\theta}\int_0^\theta \delta_\theta \, d\theta = \frac{1}{\theta}\int_0^\theta (\delta_0 + R(1-\cos\theta)) \, d\theta . \quad (1)$$

The integration of the above relation from $\theta = 0$ to $\pi/2$ yields,

$$\delta_m = \delta_0 + R\left(\frac{\pi-2}{\pi}\right) . \quad (2)$$

Also from the hypothetical sphere fig. 1-b, the radius r_s can be expressed as:

$$r_s = \sqrt{R^2 - \left(R - R\left(\frac{\pi-2}{\pi}\right)\right)^2} = 0.771\,R . \quad (3)$$

The oval flat bottom radius r_b from fig. 1-c may be $\leq R$ or $\geq R$ and will be corrected later from the experimental data by a correction factor C_f, which defined as the ratio between area of droplet lower face with radius r_s and the oval flat bottom area with radius r_b.

$$C_f = \frac{\pi r_s^2}{\pi r_b^2} = \frac{r_s^2}{r_b^2} . \quad (4)$$

Substitution eq. (4) into eq. (3) gives the relation between hypothetical spherical radius R and the oval flat bottom radius r_b as follow:

$$r_b = \frac{0.771}{\sqrt{C_f}} R . \quad (5)$$

The problem could be simplified as shown in fig. 2 to investigate the force balance, hydrodynamic vapor layer, and heat transfer mechanism.

2.1. Governing equations

2.1.1. Continuity equation
The vapor under the droplet forms approximately a cylindrical shape of outer radius, r_b, and height of δ_m as shown in fig. 2-c. It is assumed that the rate of evaporation from the droplet equals the rate of vapor outlet the cylinder of r_b, and height of δ_m, (mass balance at interface).

$$-\rho_l \frac{dV}{d\tau} = \rho_v 2\pi r_b \delta_m U_m . \quad (6)$$

The mass balance at the area of radius r and $r + dr$ with height δ_m as shown in fig. 2-b and fig. 3 gives:

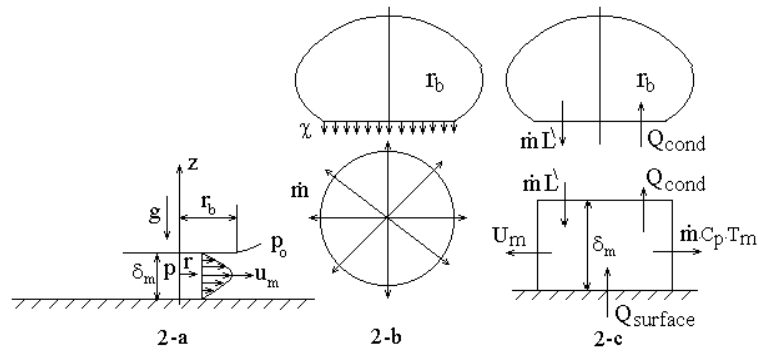$$\rho_v 2\pi r \delta_m u_m + \chi 2\pi r dr = \\ \rho_v 2\pi(r + dr)\delta_m(u_m + du_m). \quad (7)$$
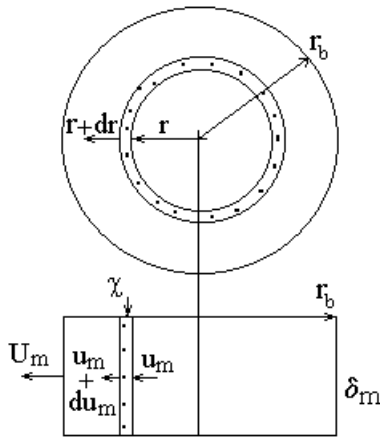
Fig. 2. Droplet evaporation with flat bottom area.

Fig. 3. Mass balance at radius of r and $r + dr$.

Where, χ is the generated vapor mass flow rate per unit area of flat bottom that penetrate perpendicularly to the area $2\pi r dr$. The value of χ is assund constant and is given as:

$$\chi = \frac{\rho_v 2\pi r_b \delta_m U_m}{\pi r_b^2} = \frac{2}{r_b} \rho_v \delta_m U_m \ . \tag{8}$$

Rearranging eq. (7) gives:

$$\chi r dr = \rho_v \delta_m (u_m dr + r du_m) = \rho_v \delta_m d(u_m r) . \tag{9}$$

Integration the eq. (9) gives:

$$\int_r^{r_b} \chi r dr = \rho_v \delta_m \int_{u_m r}^{U_m r_b} d(u_m r)$$

$$\tag{10}$$

$$\chi \frac{(r_b^2 - r^2)}{2} = \rho_v \delta_m (U_m r_b - u_m r).$$

Substituting the value of χ from eq. (8) into eq. (10), and rearranging gives the relation between the vapor mean velocity at radius r and the vapor mean velocity at radius r_b as follows:

$$u_m = U_m \frac{r}{r_b} \ . $$

(11)

2.1.2. Energy equation

It is assumed that the rate of heat transferred to the droplet by conduction equals to the heat consumed in droplet evaporation, (heat balance at interface).

$$k_v \pi r_b^2 \frac{\Delta T_{sup}}{\delta_m} = \rho_v 2\pi r_b \delta_m U_m L^{\backslash} . \tag{12}$$

Substitution of eq. (6) into eq. (12) yields,

$$-\frac{dV}{d\tau} = \frac{k_v \pi r_b^2 \Delta T_{sup}}{\rho_l L^{\backslash} \delta_m} \ . \tag{13}$$

2.1.3. Momentum equation

It is assumed that the vapor flow underneath the droplet could be approximated to a flow between 2 parallels circular discs due to the flatness of the bottom of the droplet. For steady-state laminar incompressible flow, the momentum equation with inertia terms neglected can be expressed as:

$$\frac{dp}{dr} = \mu_v \frac{\partial^2 u}{\partial z^2} \ . \tag{14}$$

The boundary conditions for vapor radial velocity; temperature and pressure under the droplet as shown in fig. 2-a are given as,

$$
\begin{aligned}
u &= 0 && at && z = 0, \delta_m \\
p &= p_0 && at && r = r_b, \ 0 \le z \le \delta_m \\
T &= T_w && at && z = 0 \\
T &= T_{sat} && at && z = \delta_m.
\end{aligned} \tag{15}
$$

The integration of eq. (14) for u is subjected to conditions of eqs. (15) gives:

$$
u = \frac{1}{2\mu_v} \frac{dp}{dr} (z^2 - z\delta_m). \tag{16}
$$

The mean radial velocity of the vapor underneath the droplet at radius r is given by:

$$
\begin{aligned}
u_m &= \frac{1}{\delta_m} \int_0^{\delta_m} u \, dz \\
u_m &= \frac{\delta_m^2}{12\mu_v} \left(-\frac{dp}{dr} \right).
\end{aligned} \tag{17}
$$

Substitution of eq. (11) into eq. (17) and considering the mean radial velocity yields:

$$
U_m \frac{r}{r_b} = \frac{\delta_m^2}{12\mu_v} \left(-\frac{dp}{dr} \right). \tag{18}
$$

Substituting of U_m from eq. (12) into eq. (18) and rearranging gives:

$$
-\frac{dp}{dr} = \frac{6\mu_v k_v \Delta T_{sup}}{\delta_m^4 \rho_v L^{\backslash}} r. \tag{19}
$$

The integration of eq. (19) using boundary conditions (15), gives the pressure distribution underneath the droplet through the vapor layer from r to r_b as follows:

$$
p - p_0 = \frac{6\mu_v k_v \Delta T_{sup}}{\delta_m^4 \rho_v L^{\backslash}} \frac{(r_b^2 - r^2)}{2}. \tag{20}
$$

2.1.4. Droplet static balance forces

The static balance forces upon the droplet as shown in fig. 2-a can be expressed as:

$$
\int_0^{r_b} 2\pi r (p - p_0) \, dr = \frac{4}{3} \pi R^3 \rho_L g. \tag{21}
$$

Substituting eq. (20) into eq. (21) and integration, one obtains the thickness of the vapor layer under the droplet as:

$$
\delta_m = \left(\frac{9}{8} \frac{\mu_v k_v r_b^4 \Delta T_{sup}}{g \rho_l \rho_v L^{\backslash} R^3} \right)^{0.25}. \tag{22}
$$

The radiation heat flux to the droplet and mass diffusion rate are examined. The value of total radiation heat to the droplet at 300 °C was found about 5.4 % of evaporation heat and the diffusion heat is guessed to be less than 2 %. So the contribution of both radiation and diffusion heat were neglected in this study. Thereafter, the heat transferred from the heated surface through the vapor layer causes the evaporation rate and decreases the droplet radius. The heat transfer rate to the droplet can be determined in steady evaporation process through small time interval (quasi-steady process).

Substitution of eq. (22) into eq. (13) as function of R yields:

$$
-4\pi R^2 \frac{dR}{d\tau} = \frac{k_v \pi r_b^2 \Delta T_{sup}}{\rho_l L^{\backslash}} \left(\frac{8}{9} \frac{g \rho_v \rho_l L^{\backslash} R^3}{\mu_v k_v \Delta T_{sup} r_b^4} \right)^{0.25}. \tag{23}
$$

Substitution of eq. (5) of r_b into eq. (23), and rearranging, one obtains a relationship between the time interval and droplet radius decrement as follows:

$$
d\tau = -\psi R^{0.25} dR. \tag{24}
$$

Where,

$$
\psi = 5.343 \sqrt{C_f} \left(\frac{\mu_v \rho_l^3 L^{\backslash 3}}{g \rho_v k_v^3 \Delta T_{sup}^3} \right)^{0.25}, \tag{25}
$$

and $L^\backslash$ is the heat required to evaporate the droplet at saturation temperature including the sub-cooling heat as follows,

$$L^\backslash = c_{p_l}(T_{sat} - T_l) + h_{fg}. \qquad (26)$$

The integration of eq. (24) for small time interval gives the change of droplet radius as:

$$\Delta\tau = \frac{\psi}{1.25}(R_1^{1.25} - R_2^{1.25}). \qquad (27)$$

Also the integration of eq. (24) from initial droplet radius, R_0, until the droplet disappears (complete evaporation) yields the droplet evaporation time. So the evaporation time of a small liquid droplet in film boiling region can be expressed as:

$$\tau_{ev} = 1.797\sqrt{C_f}\left(\frac{\mu_v \rho_l^3 L^{\backslash 3} d_0^5}{g\rho_v k_v^3 \Delta T_{sup}^3}\right)^{0.25}. \qquad (28)$$

The values of C_f for various liquid droplets were adapted by fitting the experimental data [8] with the eq. (28), and the getting values were listed in table 1. The vapor properties of tested pure hydrocarbon fuels were calculated according to the procedure explained in ref. [15]. Also, the vapor in the film between droplet and heated surface was assumed be superheated to a temperature between vapor saturation temperature and heated surface temperature.

Thereafter, the present model and above Equations are therefore believed suitable to estimate the droplet radius decrement and evaporation time of liquid droplets for water and some pure hydrocarbon fuels in film boiling region.

3. Results and discussions

To validate the predicted data of droplet evaporation time from eq. (28), a comparison was made between predicted results and the experimental data of Xiong and Yuen [8], and the comparison was illustrated in fig. 4. The predicted results of droplet evaporation time

Table 1

Experimentally derived constants C_f [8]

Liquid	Water	Hexadecane	Heptane	Decane
C_f	0.20	0.50	0.91	0.98

are seen close to a great extent of experimental findings through derivations exist depending on droplet size, surface superheating and liquid type. It was found that the mean deviation was ± 8.5 % for water droplets. The results were very close for predicted and experimental values for decane data of droplet size less than 0.5 *mm* and the deviation was estimated to be within ± 5.55 %. For hexadecane data, the prediction was very dependent on the droplets size. For droplets size less than 0.1 *mm*, the mean deviation was within ± 12 %, while for droplets size ranging from 0.1 ~ 0.4 *mm*, the mean deviation was within ± 25 %. The comparison showed acceptable agreement between prediction and experiments for heptane data with droplets size less than 0.4 *mm* and the mean deviation was within ± 30 %.

3.1. Droplet diameter decrement

Table 2 shows comparison between the experimental data of Avedisian and Fatehi [7] of evaporation time at surface temperatures of 292, 347 and 407 ℃ and droplet size ranging from 2.47 ~ 3.04 *mm*, and the prediction by eq. (28) of τ_{ev}. The average deviation between experimental data for water droplet and prediction was 3.63 %, but for heptane and decane data was 11.83 % and 14.57 %, respectively. The effects of surface superheating temperature on the evaporation time and droplet diameter decrement were illustrated in figs. 5-7. The evaporation time decreased with increasing surface superheating. The variation of droplets diameter decrement through the evaporation time were examined and compared with experimental data [7]. For water data shown in fig. 5, the trends of droplets diameter decrement showed best agreement with the experimental data. For heptane data that illustrated in fig. 6, the prediction was acceptable for the total evaporation time, but not so acceptable for the overall evaporation
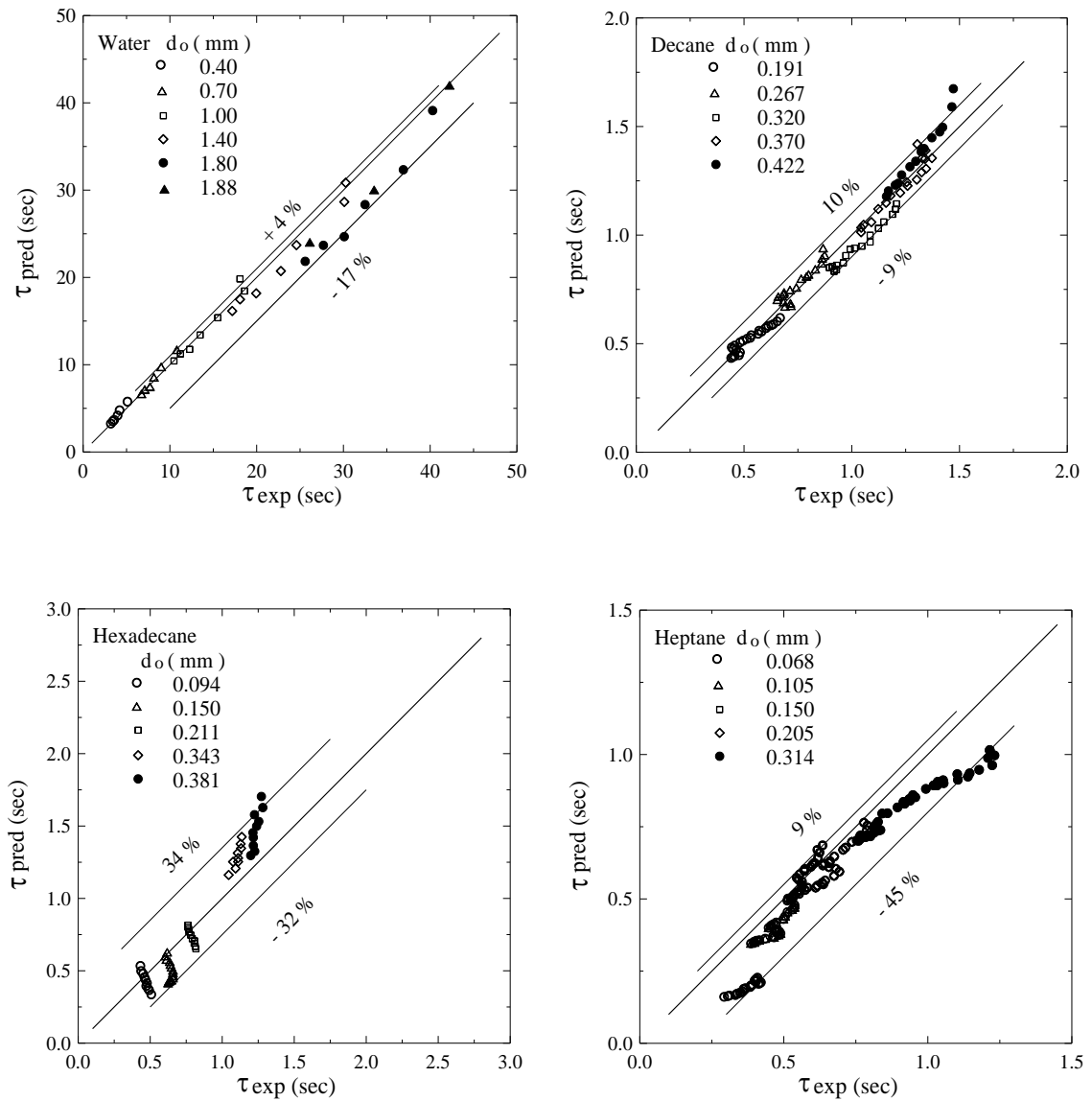
438

Fig. 4. Comparison between predicted droplet evaporation time and experimental data [8].

Table 2
Comparison between experiments [7] and prediction

Fluid	T_w (°C)	d_0 (mm)	τ_{ev} (sec) Experiment	τ_{ev} (sec) Prediction	Deviation %
Water	292	3.04	68.00	75.89	11.60
	347	2.98	60.00	60.49	00.80
	407	2.96	51.00	50.60	-00.78
Heptane	407	2.90	07.40	08.92	20.54
	292	2.73	10.20	11.44	12.16
	347	2.47	07.79	08.24	05.78
Decane	347	2.82	08.70	09.2	05.75
	292	2.80	09.25	12.74	37.73
	407	2.78	08.00	08.02	00.25
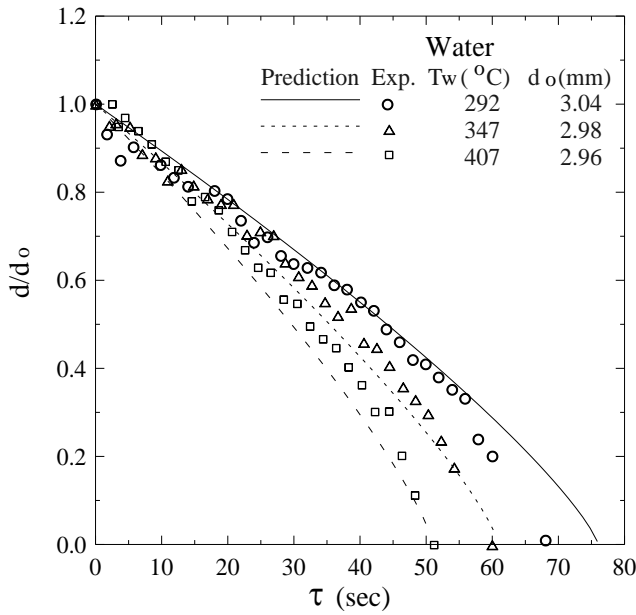
Fig. 5. Comparison between prediction and experimental data [7] for water droplet diameter decrement.
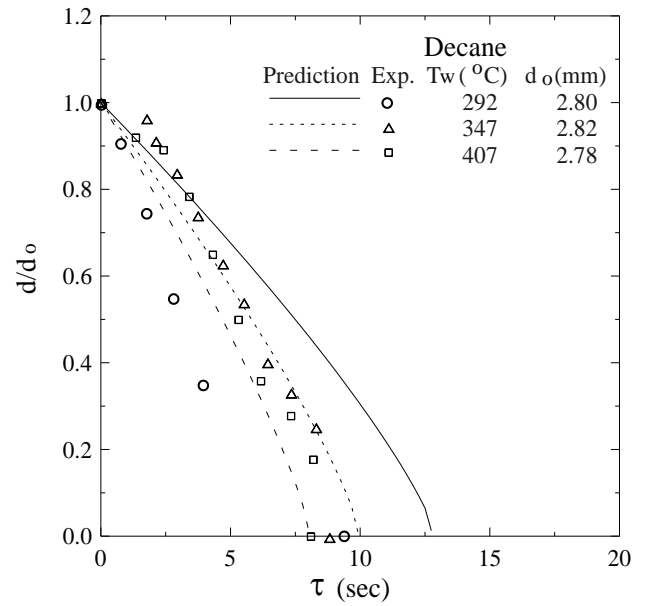

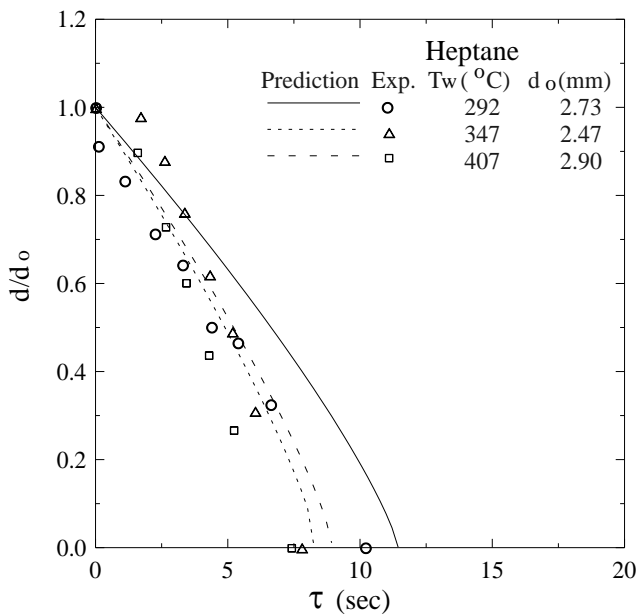Fig. 7. Comparison between prediction and experimental data [7] for decane droplet diameter decrement.

Fig. 6. Comparison between prediction and experimental data [7] for heptane droplet diameter ecrement.

history. For decane data that illustrated in fig. 7, some interference was obtained especially at the end of evaporation. The discrepancy between prediction and experimental data for hydrocarbon fuels may be due to the effects of

droplets explosion and rebounding from the surface that could practically happen at the end of evaporation. For rebounding droplets, the droplet bounces periodically from the heated surface. So, the mass diffusion and convection between the droplet and environment plays more important enhancement for total evaporation time. For these reasons, the prediction for decane data was not hugging the experimental data.

3.2. Droplet evaporation time

The comparison between the experimental data [8] of evaporation time and prediction by eq. (28) of τ_{ev} for water, hexadecane and heptane, as a function of surface temperature and droplet size was illustrated in figs. 8-10. Fig. 8 show the prediction for water data, for droplets size from 0.4 ~ 1.4 *mm,* the predicted values of τ_{ev} were less than the experimental data for large droplets because the droplet may not be in spheroid state and also due to possible explosion of the droplets. Figs. 9 and 10 show the prediction for the hexadecane and heptane data. The mean deviation between all the experimental data for tested liquid droplets and prediction was illustrated in fig. 11, and it was found that the mean deviation of the most

data was ± 35 %. The predicted results were close to the experimental findings by ± 35 % and so the comparison between prediction and experimental data was fairly well.

3.3. Droplet heat transfer

The time-average heat transfer rate from the heated surface to the hypothetical spherical droplet in film boiling region is defined as the amount of heat required to evaporate one droplet per unit area of the droplet projection, which can be expressed as,

$$q_d = \frac{2d_0 \rho_l L^{\backslash}}{3\tau_{ev}}.$$ (29)

Comparison between experimental data of Xiong and Yuen [8] for droplet heat transfer rate and prediction was illustrated in fig. 12. For water data, the relations of q_d and τ_{ev} satisfies the experimental data and the average deviation was 2 ~ 8 %. But, for heptane and hexadecane data the prediction by q_d and τ_{ev} gives pretty well agreement with the experimental data for low surface superheating, but the deviation from experimental data increased
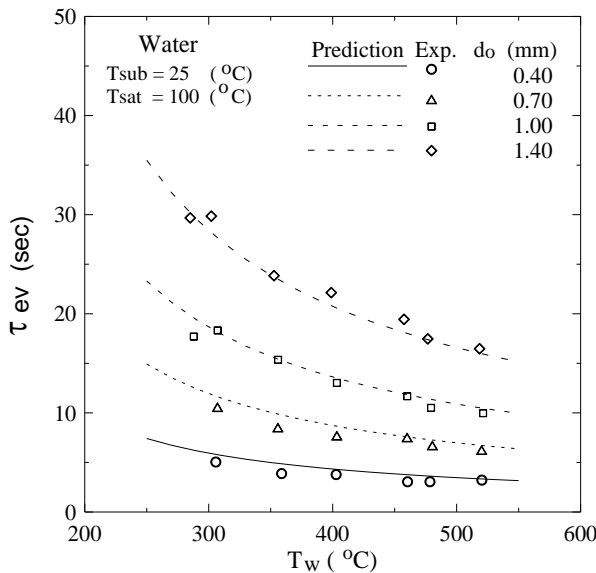

Fig. 8. Comparison between prediction and experimental data [8] for water droplet evaporation time.
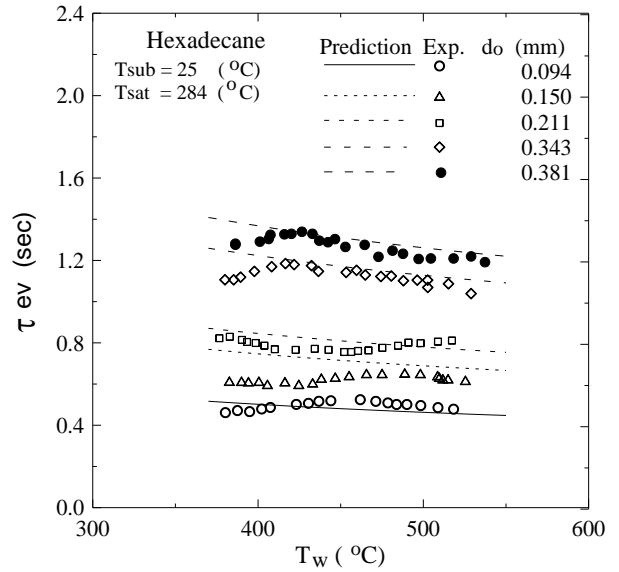

Fig. 9. Comparison between prediction and experimental data [8] for hexadecane droplet evaporation time.
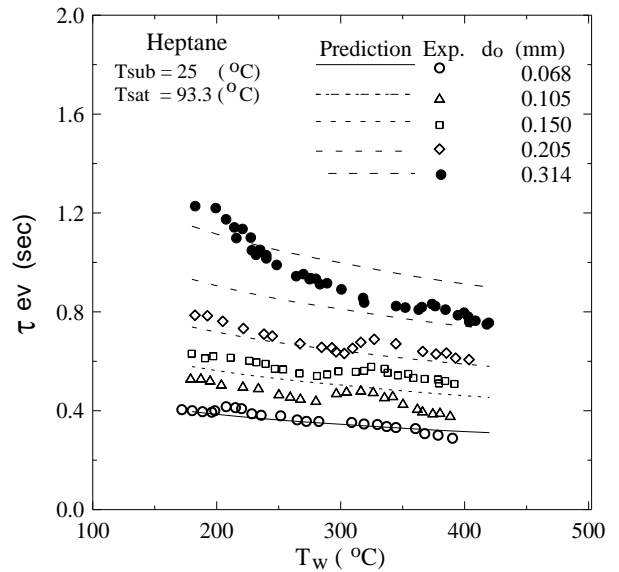

Fig. 10. Comparison between prediction and experimental data [8] of heptane droplet evaporation time.

with increasing surface superheating. The effect of droplet size on evaporation heat transfer rate for water data of Xiong and Yuen [8] and Michiyoshi and Makino [16] were illustrated in fig. 13. For small droplet diameter less than 1 mm, the prediction seems satisfy the experimental data, but for large droplet size, the prediction was less than the

experimental data by about of 12 ~ 20 %. So, the time-average droplet heat transfer rate in film boiling satisfies quite well the experimental data in the whole rang of surface temperature up Leidenfrost temperature especially for small droplets less than 2 *mm* of diameter.
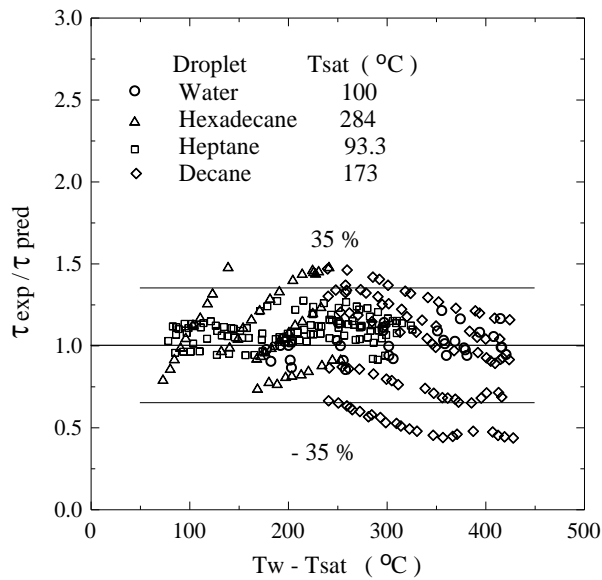

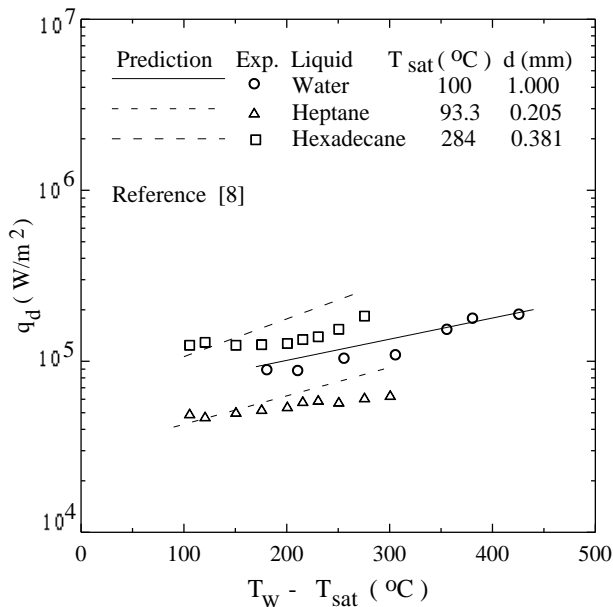Fig. 11. Deviation between experimental data and prediction.

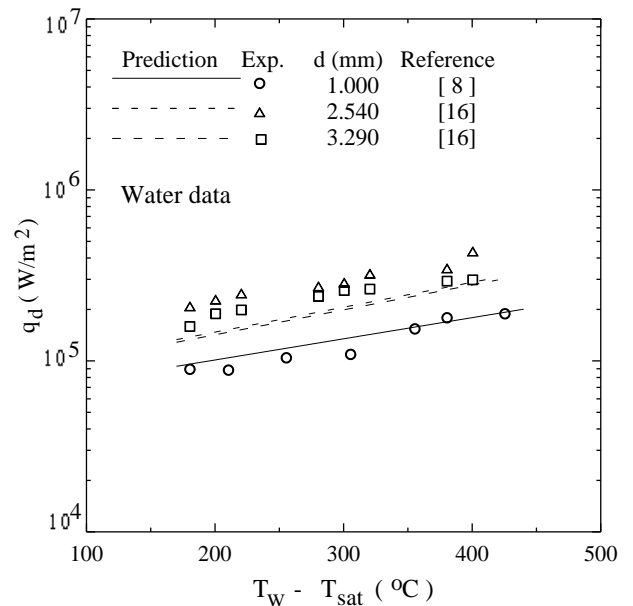Fig. 12. Comparison between prediction and experimental data [8] for droplet heat transfer rate.

Fig. 13. Comparison between prediction and experimental data for water droplet heat transfer rate.

4. Conclusions

Analytical model has been developed to predict the droplet evaporation time in film boiling region. The liquid droplet was assumed a spheroid shape with a uniform vapor gap under the droplet and the droplet bottom is at saturation temperature. The evaporation rate takes place uniformly beneath the droplet. For steady-state laminar incompressible flow, the momentum equation with inertia terms neglected, the mass balance and the energy balance at interface were solved simultaneously to obtain the droplet evaporation time. The change of droplet diameter decrement through the evaporation process was calculated and tested with available experimental data. The prediction was satisfactory for water, heptane and hexadecane data, but for decane data, some interference was observed. The droplet evaporation time was correlated and the comparison between the experimental data and prediction was fairly well for time-average droplet heat transfer rate.

Nomenclature

C_f is the area correction factor,
c_p is the specific heat [J/(kg. K),
D is the droplet diameter [m],

g	is the gravity acceleration [m/s^2],
h_{fg}	is the heat of vaporization [J/kg],
K	is the thermal conductivity [W/(m. K)],
$L^\backslash$	is the modified latent heat [J/kg],
$\dot{m}$	is the evaporation rate [kg/s],
P	is the pressure [N/m^2],
Q	is the droplet heat flux [W]
q_d	is the droplet specific heat flux [W/m^2],
R	is the droplet radius [m],
r	is the horizontal axis [m],
r_b	is the radius of droplet bottom [m],
T	is the temperature [^{o}C],
ΔT_{sup}	is the surface superheating, TW-Tsat, [K],
U_m	is the mean vapor velocity at rb [m/s],
u	is the vapor velocity at r [m/s],
u_m	is the mean vapor velocity at r [m/s],
V	is the droplet volume [m3],
Z	is the vertical axis [m],
χ	is the evaporation rate [kg/(m2.s)],
δ	is the thickness of vapor layer [m],
μ	is the viscosity [Pa. s],
θ	is the angle [o],
ρ	is the density [kg/m3],
τ	is the time [s],
τ_{ev}	is the evaporation time [s], and
ψ	is a constant.

Subscripts

0	for initial, environment,
cond	for conduction,
D	for droplet,
Exp	for experiment,
l	for liquid,
m	for mean
pred	for prediction,
sat	for saturation,
v	for vapor, and
w	for wall.

References

[1]   L.H.J. Watchters H. Bionne H.J. and Van Nouhuis, "The Heat Transfer from a Hot Horizontal Plate to Sessile Water Drops in the Spheroidal State", Chem. Eng. Sci., Vol. 21, pp. 923-936 (1966).

[2]   B.S. Gottfried C.J. Lee and K.J. Bell, "The Leidenfrost Phenomenon: Film Boiling of Liquid Droplets on a Flat plate", Int. J. Heat Mass Transfer, Vol. 9, pp. 1167-1187 (1966).

[3]   K.J. Baumeister and T.D. Hamill, Creeping Flow Solution of the Leidenfros, Phenomenon". NASA TND – 3133 (1965).

[4]   K.J. Baumeister R.C. Hendricks and T.D. Hamil, Metastable Leidenfrost States, NASA TN – 3226 (1966).

[5]   K.J. Baumeister E.G. Keshock and D. A. Pucci, Anomalous Behavior of Liquid Nitrogen Drops in Film Boiling, NASA TM X – 52800 (1970).

[6]   G.S. Emmerson, "The Effect of Pressure and Surface Material on the Leidenfrost Point of Discrete Drops of water", Int. J. Heat Mass Transfer, Vol. 18, pp. 381-386 (1975).

[7]   C.T. Avedisian and M. Fatehi, "An Experimental Study of the Leidenfrost Evaporation Characteristics of Emulsified Liquid Droplets", Int. J. Heat Mass Transfer, Vol. 31 (8), pp. 1587-1603 (1988).

[8]   T.Y. Xiong and M.C. Yuen, "Evaporation of a Liquid Droplet on a Hot Plate", Int. J. Heat Mass Transfer, Vol. 34 (7), pp. 1881-1894 (1991).

[9]   P.J. Halvorson, R.J. Carson, S.M. Jeter and S. I. Abdel-Khalik, "Critical Heat Flux Limits for a Heated Surface Impacted by a Stream of Liquid Droplets", Journal of heat Transfer, ASME, Vol. 116, pp. 679-685 (1994).

[10]   M.L. Sawyer S.M. Jeter and S.I. Abdel-Khalik, "A Critical Heat Flux Correlation for Droplet Impact Cooling", Int. J. of Heat and Mass Transfer, Vol. 40 (9), pp. 2123-2131 (1997).

[11]   G. George, S. Siang and N.P. Daniel, "Effects of Gravity and Ambient Pressure on Liquid Fuel Droplet Evaporation", Int. J. of Heat and Mass Transfer, Vol. 46 (2), pp. 283-296 (2003).

[12]   C. Lorenzo K. Suresh and M. Sohail, "A Molecular Dynamics Simulation of Droplet Evaporation", Int. J. of Heat and Mass Transfer, Vol. 46 (17), pp. 3179-3188 (2003).

[13] K. Sefiane L. Tadrist and M. Douglas, "Experimental Study of Evaporating Water-Ethanol Mixture Sessile Drop: Influence of Concentration", Int. J. of Heat and Mass Transfer, Vol. 46 (23), pp. 4527-4534 (2003).

[14] F. Elyssa and W.Z. Black, "Heat Transfer and Evaporation Rates of Small Liquid Droplets on Heated Horizontal Surfaces", Int. J. of Heat and Mass Transfer, Vol. 47 (6), pp. 1187-1200 (2004).

[15] C. Robert Reid, M. John Preusnitz and E. Bruce Poling, The Properties of Gases & Liquids, Fourth Edition, McGraw-Hill Book Company (1987).

[16] I. Michiyoshi and K. Makino, "Heat Transfer Characteristics of Evaporation of a liquid Droplet on Heated Surfaces", Int. J. of Heat and Mass Transfer, Vol. 21, pp. 605-613 (1978).